Journal of Structural Geology 32 (2010) 843–854

Contents lists available at ScienceDirect

Journal of Structural Geology

journal homepage: www.elsevier.com/locate/jsg

Magma-driven antiform structures in the Afar rift: The Ali Sabieh range, Djibouti

Bernard Le Gall [a,*], Mohamed Ahmed Daoud [b], René C. Maury [a], Joël Rolet [a], Hervé Guillou [c], Christian Sue [a]

[a] Université Européenne de Bretagne, Université de Brest, CNRS; UMR 6538 Domaines Océaniques, IUEM, place N. Copernic, 29280 Plouzané, France
[b] Institut des Sciences de la Terre, Centre d'Etudes et de Recherches de Djibouti, B.P. 486, Djibouti Ville, Djibouti
[c] UMR 1572, LSCE/CEA-CNRS, Domaine du CNRS, 12 avenue de la Terrasse, 91118 Gif-sur-Yvette, France

ARTICLE INFO

Article history:
Received 3 November 2009
Received in revised form
1 June 2010
Accepted 16 June 2010
Available online 23 June 2010

Keywords:
Afar rift
Djibouti
Ali sabieh range
Oligo-Miocene
Mafic laccolith
Antiform
Extension

ABSTRACT

The Ali Sabieh Range, SE Afar, is an antiform involving Mesozoic sedimentary rocks and synrift volcanics. Previous studies have postulated a tectonic origin for this structure, in either a contractional or extensional regime. New stratigraphic, mapping and structural data demonstrate that large-scale doming took place at an early stage of rifting, in response to a mafic laccolithic intrusion dated between 28 and 20 Ma from new K-Ar age determinations. Our 'laccolith' model is chiefly supported by: (i) the geometry of the intrusion roof, (ii) the recognition of roof pendants in its axial part, and (iii) the mapping relationships between the intrusion, the associated dyke-sill network, and the upper volcanic/volcaniclastic sequences. The laccolith is assumed to have inflated with time, and to have upwardly bent its sedimentary roof rocks. From the architecture of the ~1 km-thick Mesozoic overburden sequences, ca. 2 km of roof lifting are assumed to have occurred, probably in association with reactivated transverse discontinuities. Computed paleostress tensors indicate that the minimum principal stress axis is consistently horizontal and oriented E-W, with a dominance of extensional *versus* strike-slip regimes. The Ali Sabieh laccolith is the first regional-scale magma-driven antiform structure reported so far in the Afro-Arabian rift system.

1. Introduction

Antiform-synform structures can form in several tectonic environments, in response to either compressional or extensional stress regimes. In continental rifts, such structures usually develop over a wide range of scales. They are often associated with extensional or transfer faulting (Withjack et al., 1989; Schlische, 1995, and references therein). Alternatively, they can be connected with either salt diapirs or high-level magmatic intrusions (Rowan, 1995). Most folds described so far within the Cenozoic Afro-Arabian Rift System have been assigned to basin inversion, in response to regional and/or local compression, e.g. in the Rukwa and North Kenya rifts (Ring et al., 1992; Morley et al., 1999; Le Gall et al., 2005). Active compression is also well documented further north, in parts of the Afar rift, along individual seismogenic reverse faults that cut through the <3 Ma-old Stratoid basalts filling the Afar depression (Fig. 1a) (Hofstetter and Beyth, 2003). Contractional strain was assumed to have operated at an earlier stage of rifting in SE Afar (Clin and Pouchan, 1970) from the antiformal structure of Mio-Pliocene volcanics in the Ali Sabieh Range (ASR hereafter) (Fig. 1). However, the causal mechanisms of early compression within the overall Afar kinematic framework were not fully understood. Alternatively, the ASR was later regarded as a horst-type structure (Clin, 1991; Eagles et al., 2002).

These early interpretations of the ASR as a tectonic structure are challenged in the present work. Instead, we propose a magma-driven doming model from new geological mapping, field structural analysis, and ASTER remote sensing interpretations, combined with K/Ar radiometric dating and geochemical analyses of Oligo-Miocene mafic volcanics. The growth of the ASR is here assigned to the emplacement of a mafic laccolith in Late Oligocene-Early Miocene, under extensional stress conditions.

2. Geological setting of the Ali Sabieh range

The Afar rift system was initiated during the Oligocene with the emplacement of 30 Ma-old flood basalts, currently exposed in the Ethiopian plateau and in Yemen (Rogers, 2006). The major downthrow of the ca. 10^5 km^2 fan-shaped Afar depression (Fig. 1b) took place during extensional faulting, at 29–26 Ma, along the Ethiopian escarpment to the west (Wolfenden et al., 2005). Much more controversial are the causal mechanisms and timing of the uplift of the Ali Sabieh and Danakil ranges (DR) that limit the depression to the east (Fig. 1b and d). In these elevated areas, the tectonic style of

* Corresponding author. Tel.: +33 2 98 49 87 56; fax: +33 2 98 49 87 60.
E-mail address: blegall@univ-brest.fr (B. Le Gall).

0191-8141/$ – see front matter © 2010 Elsevier Ltd. All rights reserved.
doi:10.1016/j.jsg.2010.06.007

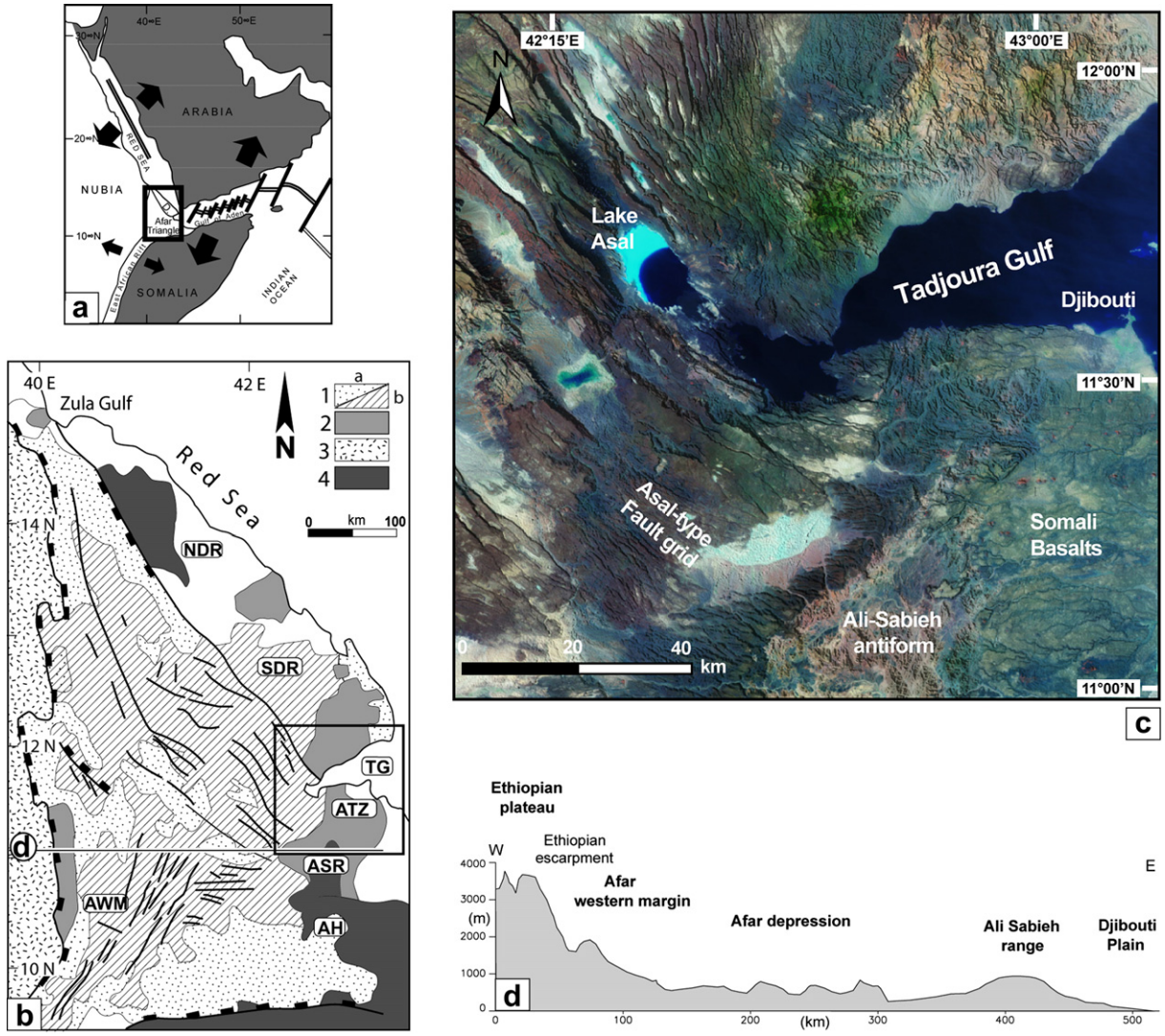

Fig. 1. Major topographical and geological structures in the Afar Triangle. (a) Plate kinematic setting of the Afar Triple Junction. Thick arrows indicate plate motion vectors and the box corresponds to the location of Fig. 1b. (b) Main geological units. 1. <3 Ma-old series in the Afar depression, 1a. Lacustrine deposits, 1b. Stratoid basalts; 2. 29–3 Ma-old synrift volcanics; 3. 30 Ma-old trap complex; 4. >30 Ma-old substratum. AH, Aisha horst; ASR, Ali Sabieh range; ATZ, Arta transverse zone; AWM, Afar west margin; NDR, North Danakil range; SDR, South Danakil range; TG, Tadjoura Gulf. The trace of the topographic profile of Fig. 1d is shown and the box is the location of Fig. 1c. (c) Landsat image showing the contrasted morphotectonic expression of the Ali Sabieh triangle-shaped antiform with respect to the Asal depression to the NW. (d) EW-oriented topographic profile across the Afar Triangle at the latitude of the Ali Sabieh range. Vertical exaggeration ~30.

Miocene synrift volcanic terranes greatly contrasts with those of younger basaltic trap-like complexes surrounding the ASR (Somali–Dalha series), and the DR (Stratoid series) (Barberi et al., 1975; Barberi and Varet, 1977).

The ASR is a 250 km^2 triangular highland that extends to the south into the Aisha horst (Fig. 1b and c) (Muller and Boucarut, 1975). Its overall map pattern is that of an eroded north-plunging antiform, cored by intrusive mafic material, and overlain by an outward-dipping envelope which includes Jurassic-Cretaceous sedimentary sequences and Tertiary volcanics (Fig. 2). Mesozoic sedimentary units are well exposed in elevated areas, as high as 1300 m in Mt. Arrey. They comprise: (1) a >350 m-thick succession of Jurassic limestones (Gasse et al., 1986) which rest unconformably over crystalline Proterozoic basement rocks, further south in Somalia (Black et al., 1972), and (2) a >500 m-thick sequence of Cretaceous fluviatile grits (Gasse et al., 1986). The Mesozoic substratum series in the ASR are in turn overlain by the effusive and volcaniclastic mafic material of the so-called Ali Sabieh magmatic complex (fully described below in terms of volcano-stratigraphy and age determinations). These early synrift volcanics, as old as Oligo-Miocene, are the youngest series involved into the Ali Sabieh antiform, since the overlying felsic sequences of the 20–9 Ma Mablas Fm (Chessex et al., 1975; Varet and Gasse, 1978; Zumbo et al., 1995; Audin et al., 2004) are assumed to post-date the onset of doming in the ASR area. The Mablas felsic volcanics are onlapped by tilted basalts of the Dalha Fm. (8.6–3.8 Ma) to the NW, and by nearly undeformed Somali basalts (7.2–3.0 Ma) to the east (Gasse et al., 1986; Deniel et al., 1994). The pre-Mablas series is intruded by a dense network of mafic-felsic sills and dykes, and all these rocks are cut by a number of regional-scale faults, with a dominant NW–SE trend (Fig. 2).

3. The Ali Sabieh mafic complex

The new volcano-stratigraphy proposed here for the ASR synrift mafic series is supported by structural and petrological data, combined with new K-Ar age determinations. Three main units are identified in the Ali Sabieh mafic complex: the main intrusion, the

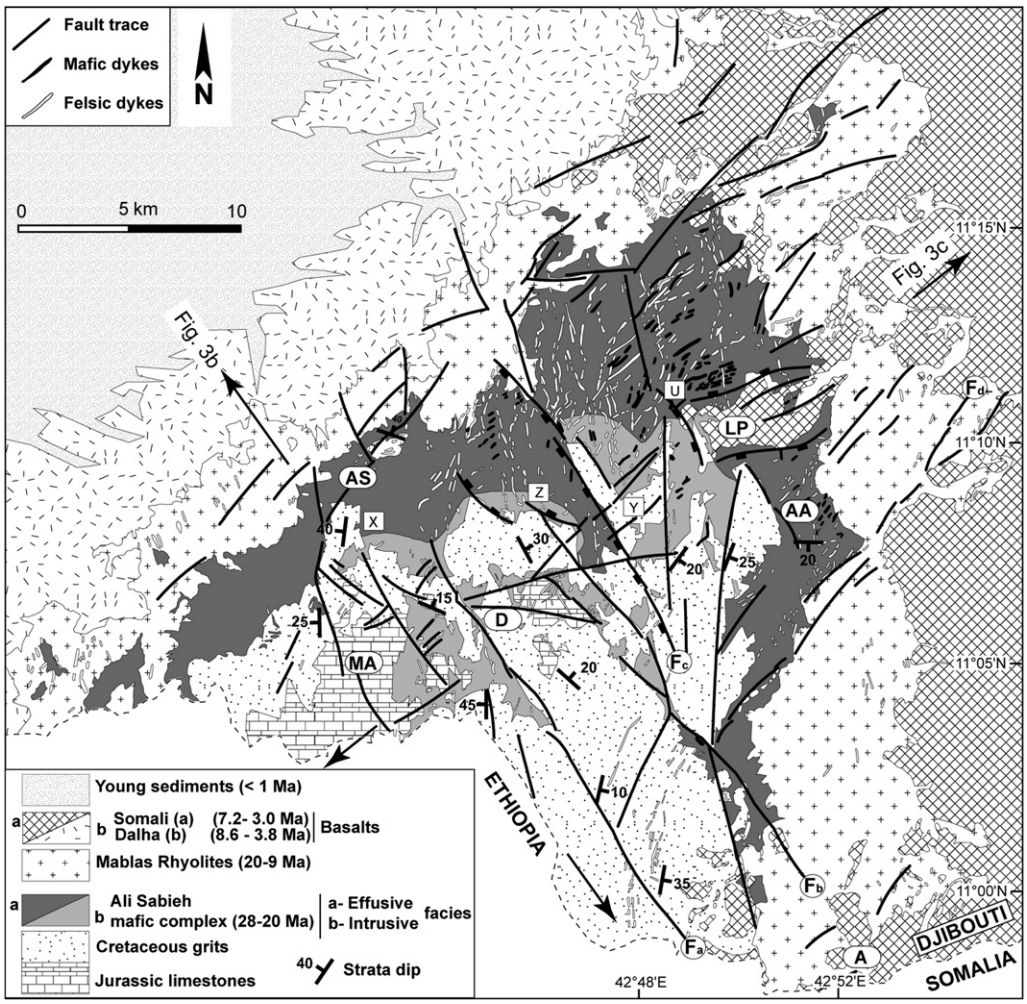

Fig. 2. Geological map of the Ali Sabieh antiform from published documents (Barrère et al., 1975; Gasse et al., 1986) with revisions from field observations and remote sensing data (ASTER) interpretation. The Ali Sabieh dyke swarm is simplified for clarity with only the thickest dykes shown to the north as topographic ridges on ASTER data. The Asal-type fault system involving the Dalha Basalts, NW of the antiform, is not shown. A, Asamo; AA, Ali Adde; AS, Ali Sabieh; D, Dadin wadi; LP, Lougag plateau; MA, Mt. Arrey. The traces of structural cross-sections shown in Fig. 3b and c are shown, as well as those of smaller-scale sections shown in Figs. 3a, 4d, 5, and 9a (X, Z, Y, and U, respectively). F_{a-d} refer to main fault structures discussed in the text.

sheet-sill-dyke network, and the subaerially-emplaced upper units (lava flows, tuffs, tuffites and volcanogenic conglomerates).

3.1. The main mafic intrusion

The strongly weathered mafic complex that extends structurally beneath the Mesozoic series in the southwestern part of the Ali Sabieh antiform (Fig. 2) was previously referred to as the Galile (Chessex et al., 1975), the Initial (Black et al., 1975), the Adolei (Barberi et al., 1975), the Ancient (Gasse et al., 1986), or the Old (Audin et al., 2004) basalts. We consider it as the main mafic intrusion of the Ali Sabieh igneous complex, the age of which is discussed below from new radiometric age determinations. In map-view, the main intrusion comprises two discrete bodies, bounded to the northeast by NW-SE-trending fault-like structures (labelled F_{a-b} on Fig. 2).

The Ali Sabieh mafic intrusive rocks show rather homogeneous aphyric textures, either microlitic or subdoleritic, with no discernible magmatic flow fabrics. The lack of internal zoning within the intrusion may be due either to the fact that the body is only exposed close to its roof or to the lack of field evidence for multiple emplacement events. While its floor is hidden, the roof of the main intrusive body is largely exposed in the crestal part of the antiform, to the SW, where its maximum exposed thickness is estimated to be ca. 400 m from observed vertical sections (Fig. 3b and c). In the Mt. Arrey area, the roof of the main intrusion forms a long wavelength arched surface, in apparent concordance with the overlying Jurassic strata (Fig. 3d). Further west, mafic intrusive materials rise abruptly to higher Jurassic stratigraphic levels, *via* step-like structures which likely represent feeder zones for the intricate mafic sheet network intruding the Mesozoic country-rocks (Fig. 3d).

3.2. The intrusive network

3.2.1. The intrusive sheet

The innermost part of the mafic unit surrounding the Cretaceous grits was previously considered as subaerial lava flows ("Basaltes fissuraux" of Gasse et al., 1986). On the basis of field observations (e.g., cross-cutting relationships, presence of sedimentary roof pendants), it is interpreted that an intrusive sheet cuts discordantly across the 'substratum-synrift sequences' boundary (Fig. 2). The structural position of the sheet, as well as its shallow attitude that is discordant with respect to the steeply-dipping Cretaceous strata

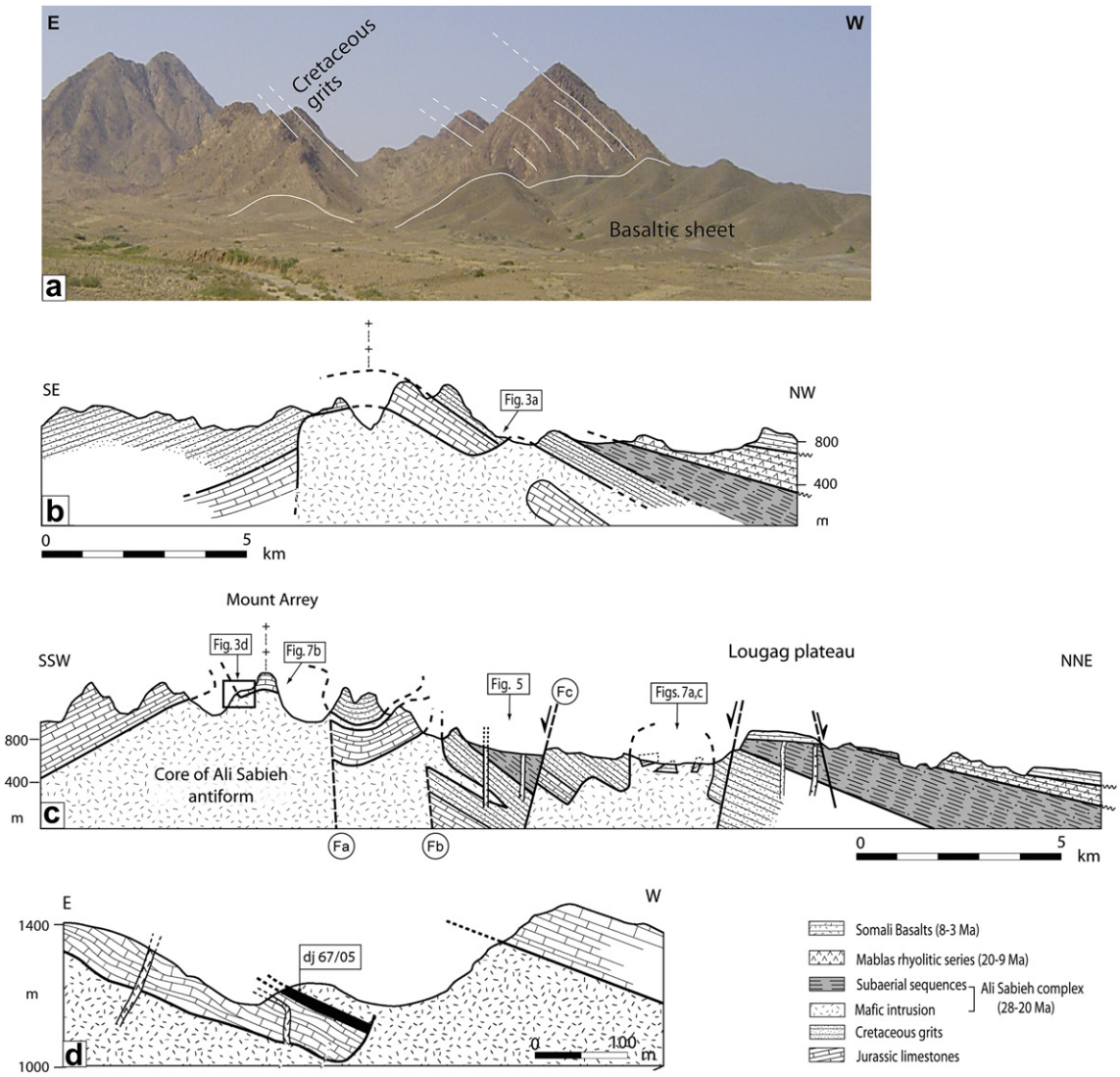

Fig. 3. Interpretative structural cross-sections of the Ali Sabieh antiform (traces shown in Fig. 2). (a) A mafic sheet from the 28–20 Ma Ali Sabieh complex, cutting discordantly through steeply-dipping (40° to the NW) Cretaceous grits on the western flank of the antiform. Location shown as X in Fig. 2. The vertical relief is ca. 150–200 m (b) NW-SE structural section, nearly orthogonal to the long axis of the antiform, showing a major step-like structure along the roof of the intrusion. Structural geometry at depth is unconstrained. (c) General NNE-SSW structural cross-section illustrating (i) the gross antiformal geometry of the ASR, (ii) vertical step-like structures (labelled F_{a-b}) along which mafic magmas possibly ascended towards progressively higher levels westwards, (iii) an extensional master fault (F_c) bounding Late Oligocene-Early Miocene half-graben volcanic infill, and (iv) the asymmetry of the antiform with a rather concordant and regular geometry of the intrusion roof on its western flank, and a much more dissected flank to the east. (d) Field cross-section close to the axial part of the antiform, in Mt. Arrey area. Note (i) the abrupt rising of mafic material to the west throughout Jurassic strata, and (ii) the presence of probably early mafic intrusions (an inclined dyke and a concordant gabbroic sill) in the dipping host-rock sequences. Location shown in Fig. 3c. Vertical exaggeration ~2. The orientation of the cross-section is as observed in the field.

(Fig. 3a), indicates that (1) it is probably the structurally highest intrusive sheet of the Ali Sabieh mafic complex, and (2) it was emplaced during doming into previously upwarped Cretaceous host-rocks.

3.2.2. The sill/dyke swarm

Despite an almost ubiquitous distribution of dykes throughout the pre-Mablas series of the ASR, one zone of increased density is observed in the Ali Sabieh effusive mafic series in the northern part of the study area (Fig. 2). There, the topographically subdued volcanic material is intruded by a closely spaced and composite (mafic/felsic) dyke network, forming narrow linear topographic ridges (Fig. 4b), with predominant NE-SW and N-S orientations (Fig. 4c) on ASTER satellite images (Fig. 4a). Field and map measurements indicate that both mafic and felsic dykes display an average width >20 m (Fig. 4d), and corresponding lengths up to a few km (Fig. 4a). Their contacts with the country-rocks are generally very steep. An emplacement mechanism by multiple injections of magma is locally suggested by the 'dyke-in-dyke' arrangement of steeply-dipping basaltic dykes on the cross-section of Fig. 4d. Further south, the tilted Mesozoic strata coring the antiform are intruded by generally narrower (<2 m-thick), and dominantly mafic dykes, in a vertical or steeply-dipping attitude. In most of cases, steeply-dipping dykes have experienced a rotation quite similar to that of their tilted host-rocks, a feature which suggests early emplacement, prior to regional doming.

3.3. The subaerially-emplaced upper sequences

On the revised geological map (Fig. 2), highly weathered mafic rocks are exposed in a topographically subdued area between the Cretaceous grits and the Mablas outer hills. Parts of these rocks

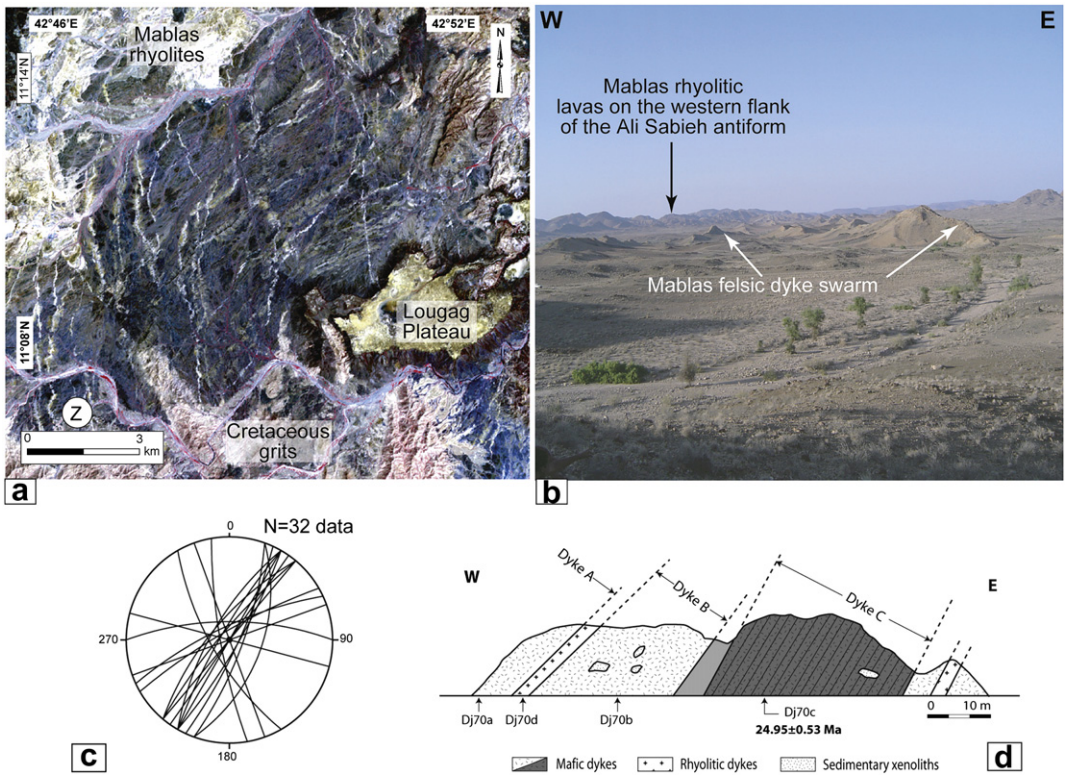

Fig. 4. The Oligo-Miocene Ali Sabieh dyke swarm. (a) ASTER remote sensing data showing the trace (white lines) of dominantly felsic dykes in the NNE termination of the antiform. Note the prominent N-S and NE-SW trends of the main dykes. Z denotes the location of the section in Fig. 4d. (b) Topographic expression of >10 m-thick felsic dykes (Mablas series) forming linear ridges through the Ali Sabieh effusive series. View towards the north from the SW part of the map in Fig. 4a. (c) Stereonet of dyke orientations (32 data measured in the field) (Wulff projection, lower hemisphere). Mafic (×26) and rhyolitic (×6) intrusions are shown together. (d) Steeply-dipping attitude (70–80° to the NW) of four mafic dykes (<20 m-thick in average, including the dyke dj70c dated at ~25 Ma), arranged in a 'dyke-in-dyke' structure, and cut by parallel and narrower felsic intrusions, probably related to the Mablas series. Location of the section shown as Z in Figs. 2 and 4a.

were assigned to either (1) the 'Basaltes fissuraux' (Gasse et al., 1986), or (2) the younger Mablas felsic series (Gadalia, 1980; Gasse et al., 1986). We consider the innermost part of this map-unit as a high-level intrusive mafic sheet of the Ali Sabieh complex. The rest of the unit is regarded as the subaerial (effusive or volcaniclastic) upper part of this complex. Its map extent varies considerably, from more than 10 km in the NE termination of the antiform to a narrow strip along the flanks of the structure (Fig. 2). The Ali Sabieh upper sequences show a homoclinal succession of bedded mafic rocks, dipping consistently 25–30° to the ENE, on the top of similarly-dipping Cretaceous grits (Fig. 5). Despite intense weathering, a number of specific volcanic and volcaniclastic facies were recognized in this sequence. They include (i) porphyritic picrobasaltic lava flows, (ii) three levels of mafic boulder-bearing

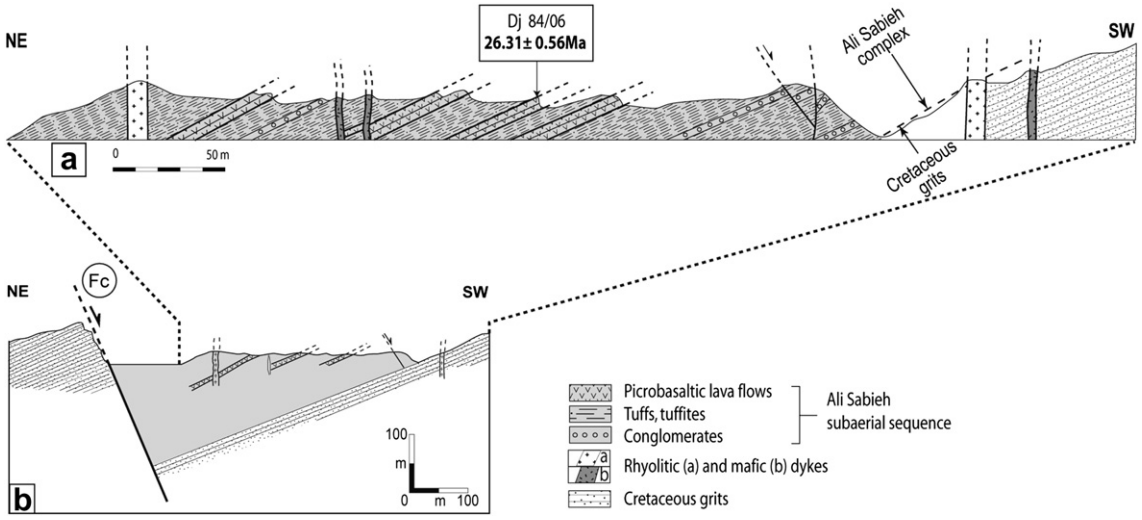

Fig. 5. Structural section across the upper mafic sequences of the Ali Sabieh complex (28–20 Ma). (a) Exposed section showing the concordant dipping attitude of both the underlying Cretaceous grits and the Oligo-Miocene volcanic basin infill. Sample dj84/06 is a picrobasaltic lava flow which yielded a K/Ar age of ~26.3 Ma (see paragraph 3.4). Location shown as Y in Fig. 2, and on the regional cross-section in Fig. 3c. (b) Interpreted structural section implying a syn-volcanic half-graben basin, facing to the west.

Table 1
Unspiked^{40}K-^{40}Ar age determinations on basaltic samples from the Ali Sabieh Oligo-Miocene volcanic complex (see Appendix 2 for sample locations). Analytical methods described in the text. Ages were calculated using the constants recommended by Steiger and Jäger (1977).

Sample Experiment	Split K (wt%) ±1σ	Mass molten (g)	^{40}Ar*%	^{40}Ar* 10^{-11} (mol./g) ±1 σ	Weighted mean ^{40}Ar* 10^{-11} (mol./g) ±1 σ	Age (Ma) ±2<σ
dj92/06						
7419	0.672 ± 0.007	1.14897	59.555	2.342 ± 0.012		
7435		1.03413	54.852	2.356 ± 0.012	2.348 ± 0.008	20.04 ± 0.42
dj85/06						
7486	1.515 ± 0.012	1.02570	59.789	5.208 ± 0.026		
7519		0.53711	56.960	5.400 ± 0.027	5.301 ± 0.019	20.06 ± 0.42
dj62/05						
7258	0.728 ± 0.007	0.44500	37.935	2.932 ± 0.015		
7274		0.48997	39.211	2.969 ± 0.015	2.950 ± 0.011	23.22 ± 0.49
dj70/05c						
7251	0.623 ± 0.006	0.97913	30.598	2.692 ± 0.014		
7267		1.18979	32.084	2.738 ± 0.014	2.715 ± 0.010	24.95 ± 0.53
dj84/06						
7453	0.132 ± 0.001	1.01047	12.897	0.605 ± 0.032		
7469		1.04650	12.251	0.609 ± 0.033	0.607 ± 0.022	26.31 ± 0.56
dj124/05						
7276	0.666 ± 0.007	1.16157	48.359	3.231 ± 0.016		
7292		0.60841	49.543	3.218 ± 0.016	3.225 ± 0.011	27.71 ± 0.58

conglomerates interpreted as lahar deposits, and (iii) fine-grained tuffs and tuffites which form the bulk of the section. Vertical basaltic and rhyolitic dykes, trending either NS or NW-SE cut the succession, and might belong to the above-mentioned composite dyke network. Owing to the lack of significant faults in the section, the thickness of the exposed volcanic and volcaniclastic series is estimated to be ca. 200 m. In map-view, this unit is bounded to the east by a 20 km-long elongate uplifted fault block of Cretaceous grits, trending NW-SE (Figs. 2 and 5a). The unit is believed to lie within a narrow SW-facing half-graben basin filled up with synrift volcanics, and controlled to the east by a master fault (labelled F_c on Figs. 2 and 5a).

Further NW, in the Ali Sabieh town area (Fig. 2), stratigraphically higher picrobasaltic lavas form several meter-thick flows, dipping gently (~20°) to the north. The lack of accurate strata dip measurements in the exposed part of the Ali Sabieh volcanic/volcaniclastic sequence precludes any accurate estimate of its total thickness. However, this thickness might be less than 500 m based on an interpretation of the regional geology (Fig. 3).

3.4. ^{40}K–^{40}Ar radiometric dating

With the exception of one microgabbro (sample dj67/05 on Fig. 3d section), the ASR igneous rock samples are picrobasaltic and

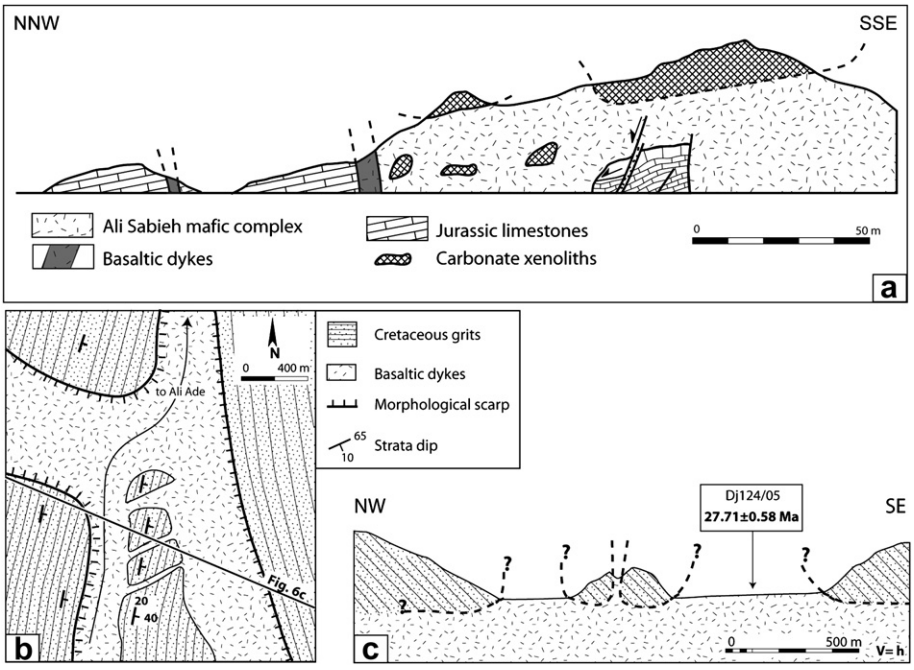

Fig. 6. Various types of sedimentary country-rocks inliers within the Ali Sabieh Oligo-Miocene mafic intrusive complex. (a) Xenoliths (meter-scale) and rafts (>10 m) of Jurassic limestones surrounded by mafic magma. The steeply-dipping basaltic dyke to the NNW is located along a step-like contact between the main intrusion and a gently dipping (probably authochtonous) limestone succession (see text for details). Location: west of the laccolith coring the antiform. (b, c) Map and cross-section of totally disconnected Cretaceous country-rock bodies, still displaying a preserved parallel bedding, and separated by an intricate sill-dyke network. These *in situ* rafts might originate from the progressive disruption of an initially homogeneous sedimentary cover by a propagating and inflating magma-filled fracture system. Location of Dadin wadi area shown in Fig. 2.

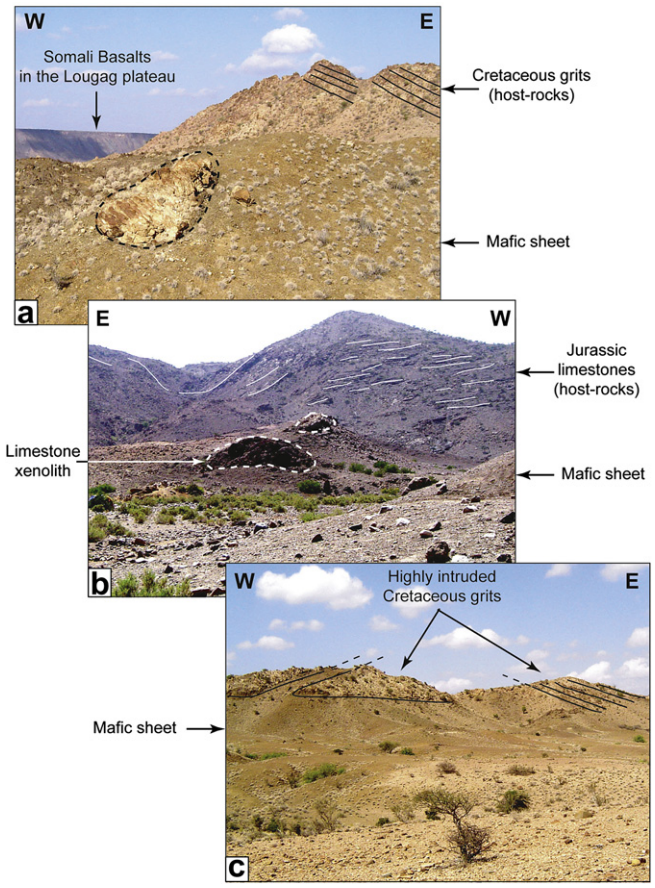

Fig. 7. Photographs of Mesozoic sedimentary xenoliths embedded within the Ali Sabieh Oligo-Miocene mafic complex (see location on the cross-section in Fig. 3c). (a) A ~10 m-large block of Cretaceous grits enclaved within the structurally highest mafic sheet of the intruding complex. Note the autochtonous east-dipping Cretaceous strata in the back of the exposed section. (b) Meter-size inliers of both Jurassic limestones and Cretaceous sandstones in the axial part of the laccolith. The dominantly east-dipping limestone strata in the back of the photograph (underlined as white lines) represent the structurally highest country-rock units in the axial part of the antiform. (c) Closely-spaced bodies of Cretaceous grits separated by a mafic sill-dyke network displaying sharp and linear intrusive contacts. (Same location as Fig. 7a).

basaltic lavas. The major and trace element compositions of 13 samples are given in the Electronic supplement (Appendix 1; analytical methods described in Cotten et al., 1995). They are transitional basalts with a dominant tholeiitic tendancy (Barberi et al., 1975; Gasse et al., 1986; Vidal et al., 1991; Deniel et al., 1994). Six ASR mafic rocks, including three dykes and sills and three lava flows (locations given in the Electronic supplement, Appendix 2), have been dated. Unspiked K-Ar experiments were carried out at the 'Laboratoire des Sciences du Climat et de l'Environnement' (Gif-sur-Yvette), on purified aliquots of microcrystalline groundmass (Cassignol and Gillot, 1982; Yurtmen et al., 2002; Guillou et al., 2004; Scaillet and Guillou, 2004). The volumetric calibration of the spike-free introduction line (Charbit et al., 1998) allows Ar content to be determined with a precision of 0.2% ($\pm 2\sigma$). The samples yield ages ranging from 27.71 ± 0.58 Ma to 20.04 ± 0.42 Ma (Table 1), and the age ranges of the three intrusions and the three lava flows clearly overlap. These ages are in agreement (i) with previous whole-rock K-Ar ages of Ali Sabieh basalts (26.7 ± 1.0 and 20.0 ± 0.6 Ma; Barberi et al., 1975; Black et al., 1975; Chessex et al., 1975, 1979), and (ii) with one $^{40}Ar/^{39}Ar$ plateau age of 23.6 ± 0.5 Ma (Zumbo et al., 1995). However, these mutually consistent results do not necessarily mean that the emplacement of the ASR mafic complex lasted 8 My, an unusual time span even for a large intrusion or shallow intracrustal magma chamber (Petford et al., 2000; Annen et al., 2006). Indeed, minor hydrothermal alteration might lead to significant deviations of the apparent ^{40}K-^{40}Ar ages with respect to their magmatic emplacement ages. A good example of such disturbance of the K-Ar clock due to hydrothermal alteration is provided by our test experiments carried out on the microgabbroic sill (dj67/05), which contains hydrothermal minerals (chlorite, epidote, pyrite), and accordingly displays a relatively high Loss On Ignition value (4.38 wt.%). For this sample, an apparent ^{40}K-^{40}Ar age of 16.45 ± 0.50 Ma is obtained (shown in Appendix 2, but not in Table 1). This age is not consistent with the geological position of the microgabbro, and therefore is not the emplacement age.

4. New clues to the structure of the Ali Sabieh antiform

4.1. Insights from sedimentary xenoliths within the Ali Sabieh intrusions

The contacts between the Ali Sabieh basaltic intrusions and their country rocks are almost invariably sharp. Narrow thermal metamorphic aureoles are commonly observed in the host-rocks, with minor baking effects within a few meters of the contact of the main intrusion. However, there is no field evidence for the occurrence of assimilation processes. We have identified numerous isolated large xenoliths of sedimentary rocks, totally surrounded by igneous material, within the main intrusive body of the Ali Sabieh complex (Figs. 6 and 7). Most of these sedimentary xenoliths are located within or close to the (eroded) roof zone of the intrusion. Their sizes range from a few m^3 to tens of m^3, and their local origin is attested by lithological similarities with the adjacent autochtonous Jurassic (limestones) and Cretaceous (grits) successions. Xenoliths with relatively modest sizes, less than a few m^3, show irregular shapes. They generally occur as randomly oriented slabs with preserved sedimentary layering, totally discordant from one xenolith to another, and also with respect to those of adjacent autochtonous strata (Figs. 6a and 7a,b). They typically resemble roof pendants which sank, with or without rotation, into the magma at one stage of its emplacement. By contrast, much larger sedimentary slabs (up to tens of m^3) form closely-spaced bodies displaying sharp and linear contacts with the igneous material (Fig. 6b and c). Bedding in many of these sedimentary bodies exhibit remarkably uniform strike and dip, which might be inherited from their original position. This observation implies that significant differential motions between sedimentary blocks did not occur during the intrusion process (Fig. 7c).

4.2. Geometry and timing of emplacement

The general map pattern and dips (77 field measurements) of the pre-Dalha/Somali series characterize an asymmetrical fold-like structure, plunging toward the NNE, and displaying a much wider and more structurally complex flank to the east (Fig. 2). Strata dip values range from 0 to 45°, and cluster at ca. 20° (Fig. 8a). The greatest values correspond to east-dipping strata from the eastern flank. However, bed dips as large as 45° are locally observed on the western flank in close association with drag-folds along strike-slip faults. Most dip measurements were obtained on Mesozoic strata (×67), and the restricted number of data from the synrift extrusive sequences (×10) does not allow us to compare rigorously the overall structure of the ca. 28–20 Ma Ali Sabieh (mafic) series, and those of the 20–9 Ma Mablas (felsic) units. However, the smaller dips (5–10°) measured for the younger (Mablas) sequences, with respect to the steeper (20–40°) Ali Sabieh series, argue for an angular unconformity within the Miocene section in the ASR area.

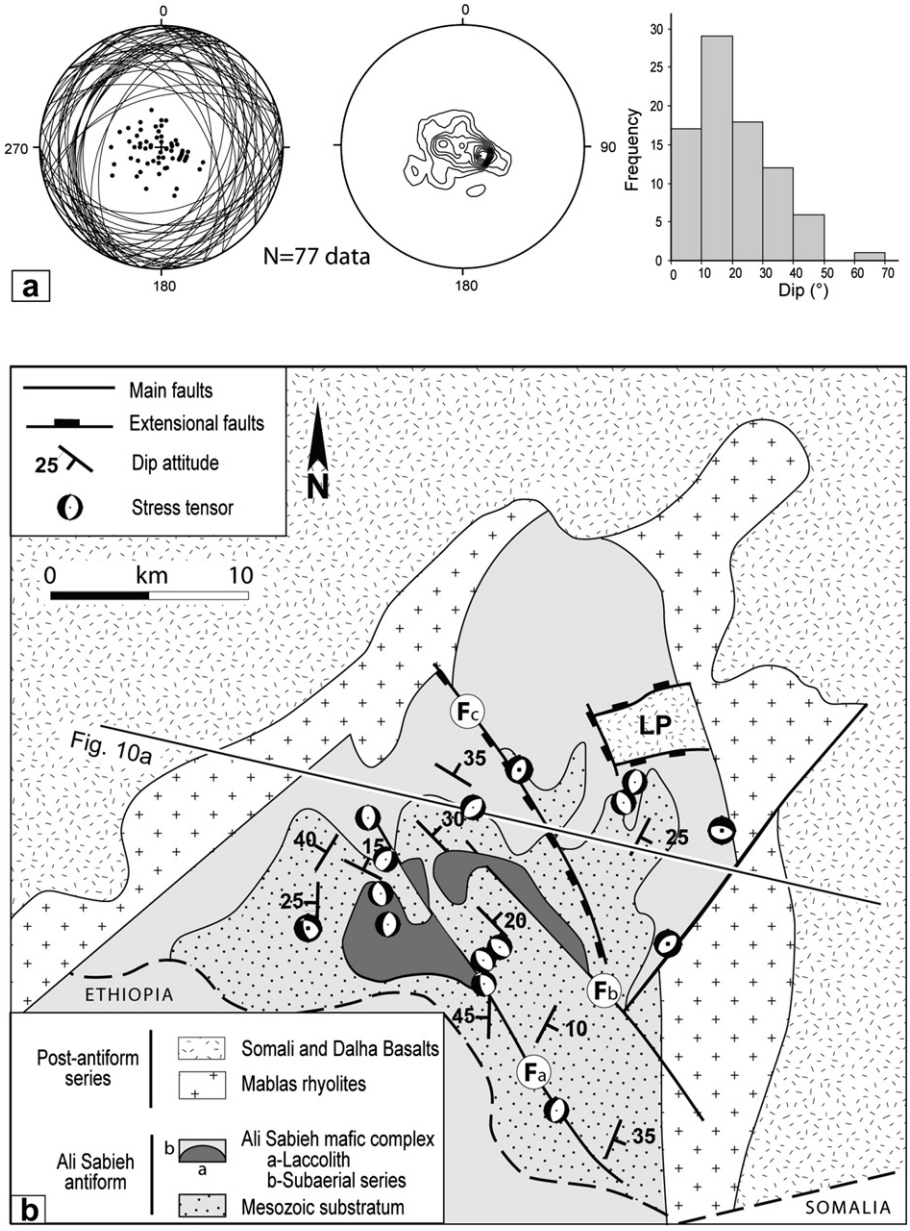

Fig. 8. Main structural features of the Ali Sabieh antiform. (a) Stereographic projection (Wulff projection, lower hemisphere) and histogram of strata dips in synrift volcanics (Ali Sabieh and Mablas Fms.) and pre-rift (Mesozoic) sequences involved in the Ali Sabieh antiform (77 data, undifferentiated). Poles and cyclographic traces of strata typically suggest a fold structure with a majority of dips in the range 15–45°. (b) Sketch structural map of the Ali Sabieh antiform showing (i) the main fault pattern ($F_{ab,c}$), (ii) the distribution of strata dips, and (iii) paleostress tensors (from 15 selected sites of measurements) typical of an extensional regime (the corresponding principal stress axes are depicted on Fig. 9c).

This interpretation is consistent with mapping results on the eastern flank of the antiform. There, the Ali Sabieh upper (volcanic/volcaniclastic) series disappear progressively southward up to Asamo, where the overlying Mablas rhyolites rest directly over Cretaceous strata (Figs. 2 and 8b). The inferred regional-scale intra-Miocene unconformity likely resulted from the eruption of Mablas rhyolitic lavas and pyroclastic flows over previously tilted mafic sequences. The modest dip of the Mablas sequences might result from their deposition over a preserved flank topography. On the other hand, the apparent conformity of the Ali Sabieh mafic sequences over the top of Cretaceous grits (Fig. 5) further indicates that (i) the earliest synrift volcanics in the ASR were emplaced as nearly-horizontal flows over a flat-lying pre-rift land surface, and (ii) the Mesozoic substratum series had not undergone an earlier (pre-rift) compressive event in contradiction with previous models (Barrère et al., 1975).

These relative timing constraints suggest that the onset of strain in the ASR occurred prior to the Mablas magmatic event, and probably during the Ali Sabieh mafic activity (28–20 Ma).

4.3. Regional fault pattern

Interpretation of ASTER remote sensing data in the ASR shows a dominantly NW-SE-oriented brittle-style fault array, oblique to the NNE-SSW axis of the antiform and crossing through the Ali Sabieh mafic complex and its Mesozoic host-rocks (Figs. 2 and 8b). One of the NW-SE transverse faults (F_c) is regarded here a as a major half-graben-bounding structure, coeval with the Ali Sabieh effusive event (Fig. 5a). Two additional parallel fault-like structures, ca. 20 km-long (labelled $F_{a,b}$), bound to the east two map-scale bodies of mafic material. They limit asymmetric steep-sided

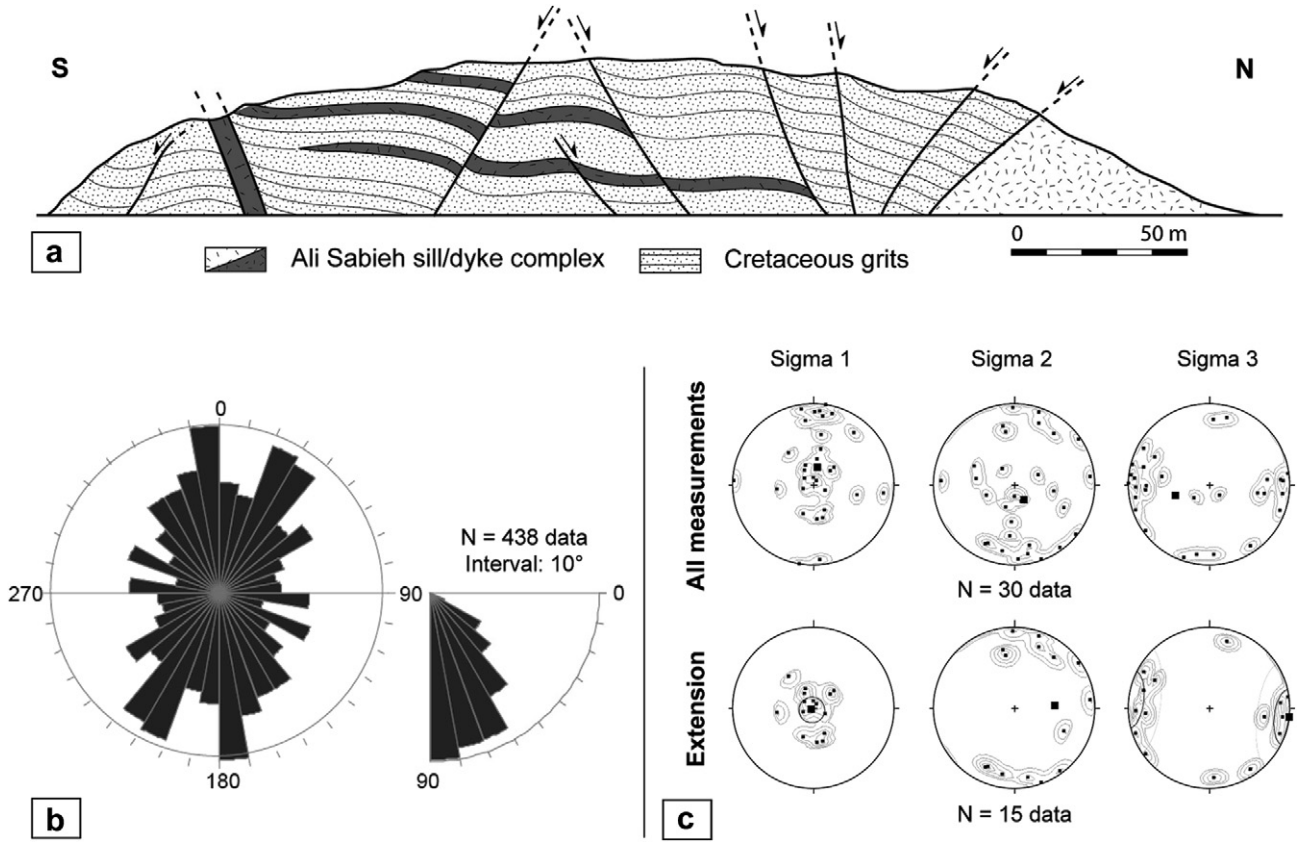

Fig. 9. Fault data and computed paleostress axes in the Ali Sabieh antiform. (a) Typical 2D fault arrangement observed in the field, showing a conjugate network of extensional faults in slightly tilted Cretaceous grits and a mafic sill-dyke swarm. Sill offsets indicate dip-slip displacements of ~10 m across most of individual faults. Location shown as U in Fig. 2. (b) Rose diagrams of strike (left) and dip (right) of 438 striated fault planes measured in the field. (c) Orientation of reconstructed principal stress axes for all measurements (30 tensors, top) and for extensional regimes (15 tensors, bottom). See text for discussion.

intrusions, rising to progressively higher levels westwards, up to the apex of the dome in the Mt. Arrey area (Fig. 3c).

NW-SE-trending brittle faults are also observed in the field as smaller-scale extensional structures cutting, with minor displacement (typically <10 m), through Mesozoic host-rocks and their intruding mafic dyke-sill swarm (Fig. 9a). They are generally spatially associated with NE-SW structures that are probably conjugate. Fault measurements (438 data) in Mesozoic (×243), Ali Sabieh (×137), and Mablas felsic (×58) rocks indicate two main modes of fault strikes at N-S and NE-SW (Fig. 9b), i.e. nearly parallel to the composite dyke swarm intruding the Ali Sabieh effusive series in the northern termination of the antiform (e.g. Fig. 4c). Fault dips range from 90° to 40°, with 65% of fault dips >60° (Fig. 9b).

The dynamic analysis of fault-slip data (Sperner et al., 1993; Angelier, 1994) led us to compute 30 tensors in Mesozoic rocks (×17), Adolei mafic volcanics (×10), and Mabla felsic intrusions (×3), respectively. According to our tensor determinations, σ_3 axes are consistently horizontal, with an E-W direction, whilst the maximum principal stress σ_1 is either subvertical (15 tensors typical of a pure extensional regime, Fig. 8b and 9c), or sub-horizontal (15 tensors typical of a strike-slip regime). Our results definitely exclude dominantly horizontal compressive stress conditions in the ASR during the onset of doming, in contrast with previous interpretations (Clin and Pouchan, 1970). One should note that a majority (10 data) of strike-slip tensors were measured close to regional transverse faults, striking either NW-SE (7 tensors) or NE-SW (3 tensors), hence suggesting local $\sigma_{1/2}$ permutations in the vicinity of probably reactivated pre-existing discontinuities.

The network of NS-oriented intrusions in the Ali Sabieh composite feeder dyke swarm is nearly orthogonal to the direction of regional extension and it likely formed as Mode I magma-filled fractures. Their pattern suggests that mafic magmatic activity and brittle extensional faults occurred simultaneously in the ASR during Late Oligocene-Early Miocene times.

Further timing constraints for the onset of faulting in the ASR area are supplied by the map distribution of the regional-scale fault network. First, the fact that the NW-SE-trending fault pattern dissecting the antiform does not transect the Mablas rhyolitic series on the outer rim of the fold structure suggests that it formed during a late stage of the emplacement of the Ali Sabieh mafic laccolith prior to the Mablas volcanic event. On the other hand, the arrest of younger extensional Asal-type faults within the Dalha–Stratoid basaltic cover, onlapping the western flank of the antiform (Fig. 1c), demonstrates that (i) the ASR area later behaved as a tectonically stable domain during younger rift stages, and that (ii) the NW-SE fault system was not reactivated.

5. A magma-driven uplift model for the origin of the ASR

Although it is often difficult to discriminate the tectonic effects of an intrusion from those of regional deformation, the magma-driven origin of the Ali Sabieh antiform is argued below from the following structural evidence. First, a compressional origin for the ASR is inconsistent with paleostress reconstructions, which instead favour either pure extensional or strike-slip conditions during the onset of magmatism in the ASR. In addition, the previous interpretations of the Ali Sabieh antiform as a regional-scale horst structure (Clin, 1991; Eagles et al., 2002) are contradicted with the observation that basement/synrift highs in the ASR are not spatially linked to clear fault rift shoulders, and more generally to any

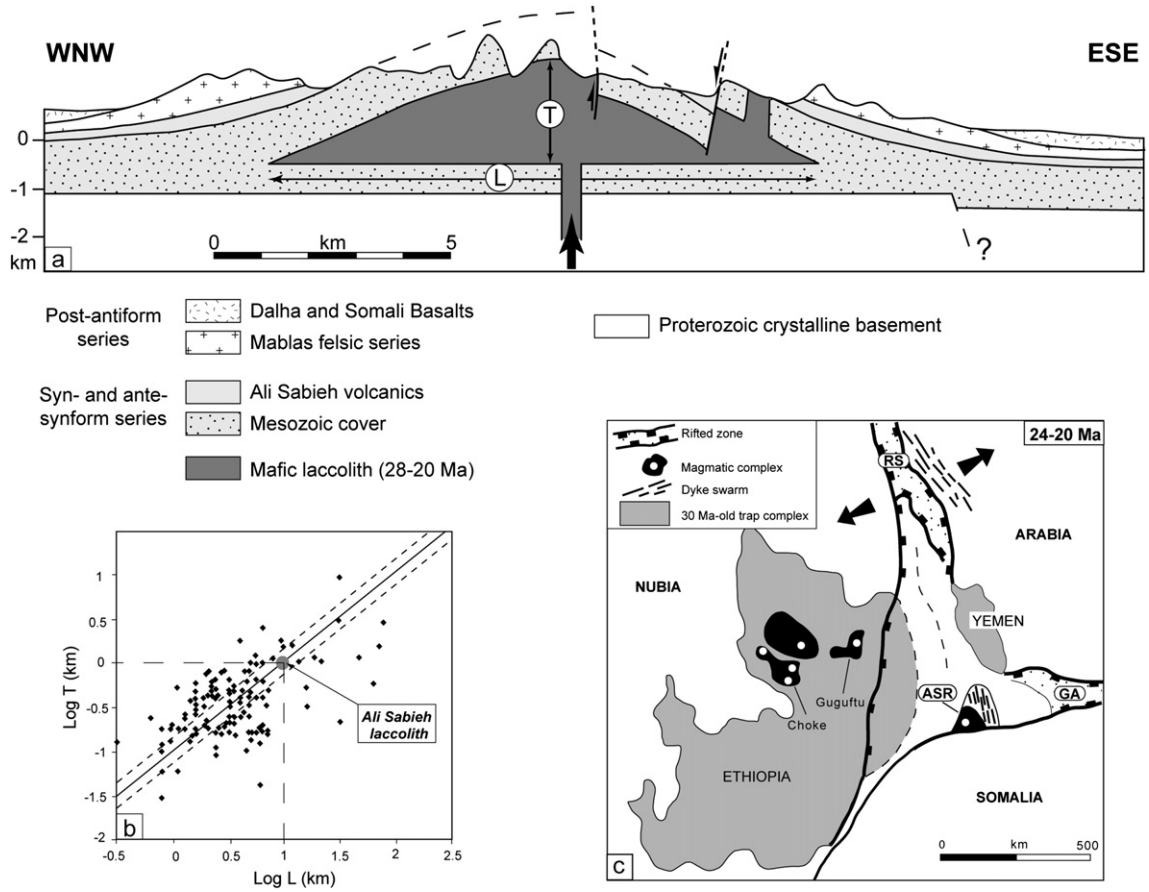

Fig. 10. Structural and geometrical characteristics of the Oligo-Miocene Ali Sabieh mafic laccolith. (a) Diagrammatic cross-section illustrating the restored geometry (before erosion) of the antiform and its coring laccolith in a magma-driven model. The geometry and dimensions of the laccolith (length (L), thickness (T) and corresponding depth of its basal contact) are not accurately constrained. The Ali Sabieh mafic dyke swarm is not drawn. Vertical exaggeration ~1.5.). (b) Log T (thickness) *versus* Log L (length) diagram for laccolith intrusions. A thickness of ca. 2 km is deduced from the estimated length value (10 km) proposed in the text for the Ali Sabieh laccolith. The thick solid black line corresponds to the best-fit slope, and the two dashed lines are the 95% confidence limits, according to Corry (1988), McCaffrey and Petford (1997), and Cruden and McCaffrey (2001). (c) Plate reconstruction of the Afar rift system at 24–20 Ma showing the position of the Ali Sabieh magmatic area (i) at the eastern periphery of the (earlier) Ethiopian flood province, and (ii) in the southern continuation of the incipient Red Sea rift and its associated axial dyke swarm (modified from Bosworth et al., 2005). ASR, Ali Sabieh range; GA, Gulf of Aden; RS, Red Sea.

extensional map-scale fault structures. The few synrift extensional faults are either local structures associated to the Ali Sabieh lava-filled half-graben, or alternatively younger structures that bound the uplifted Somali Basalts in the Lougag plateau area (Fig. 8b), and thus largely post-date the antiform.

Moreover, the magma-driven origin proposed here for the arched geometry of the Jurassic-Cretaceous sedimentary cover at the apex of the Ali Sabieh intrusion is consistent with the results of experimental modelling of high-level magma emplacement beneath overburden layers (Roman-Berdiel et al., 1995). Although the present erosion level in the ASR area precludes a precise location of the base of the main coring intrusion, the finite geometry of the Ali sabieh antiform is depicted on the diagrammatic cross-section shown in Fig. 10a. The overall asymmetry of the antiform is marked by the step-like geometry of the intrusion roof on its much more intricate eastern flank.

This section is nearly orthogonal to the NNE-SSW axis of the NNE-plunging antiform and is constructed with the following assumptions: (i) The total thickness of the Mesozoic overburden (ca. 1000 m) is nearly constant laterally. (ii) From map arrangement, and regional strata dip attitudes, the Ali Sabieh effusive series is <500 m-thick on the preserved limbs of the antiform. Its thickness is likely to decrease laterally outward, away from the feeder intrusive complex coring the antiform. (iii) From these thickness estimates, the Proterozoic/Mesozoic undeformed interface should lie at a depth of approximately 1.5 km beyond the antiform. It might continue horizontally, at a constant level, beneath the antiform. To establish the length (L) of the underlying intrusion, additional geometrical constraints are supplied by the dipping attitude of the synrift overburden. On the basis of exposed geology alone, it is difficult to determine exactly where the limbs of the antiform terminate beneath the Mablas unconformable felsic series. However, the decreasing dip attitude of the Mablas lavas and pyroclastic flows from 5 to 10° on the eastern edge of the antiform to nearly horizontal in the Goubetto area, 5 km NE of the flank of the antiform (Fig. 10a), suggests that the Ali Sabieh antiform does not extend laterally far beyond its present map exposure. Assuming a symmetrical dip pattern for the western flank of the structure would lead to estimate a maximum width of ca. 15–20 km for the Ali Sabieh antiform, and its underlying intrusion (Fig. 10a). On a Log T-Log L diagram, the maximum width value estimated above for the Ali Sabieh laccolith lies out of the main range of published data (Fig. 10b). Although more accurate geometric data are needed to better constrain the width of the Ali Sabieh laccolith, a smaller width of ca. 10 km is more likely (A.R. Cruden, personnal communication), and would better fit within the Log T-Log L diagram. That in turn indicates (i) a thickness value in the range 0.6–1.6 km, close to the thickness drawn in the section (Fig. 10a), and (ii) an aspect

ratio (amplitude/diameter) typical of laccolithic intrusions (Dixon and Simpson, 1987; Corry, 1988; McCaffrey and Petford, 1997). In addition, the assumption of a regular arch-shaped geometry for its outermost envelope would indicate ca. 1 km of erosion in the axial part of the antiform since the Lower Miocene (post-Ali Sabieh magmatism).

Considering this scenario, a few assumptions are tentatively proposed for the kinematics of emplacement of the Ali Sabieh laccolith. The generally concordant nature of the main mafic intrusion underlying the Ali Sabieh antiform suggests that the intrusion originated as a sill, and then expanded into a laccolith, flexing the Mesozoic overburden. The lifting of the intrusion roof was probably assisted by the rejuvenation of pre-existing (NNW-oriented) discontinuities. These steep structures might have guided the ascent of mafic magma at higher structural levels in the uppermost crust, whilst large portions of the sedimentary cover were concomitantly displaced in a step-wise fashion over the roof of the laccolith. The preferred location of locally-derived cover xenoliths, or roof pendants, near the roof of the intrusion might result from the downward collapse of the brittly fragmented roof, over the center of the laccolith. Such a process has been demonstrated by experimental modelling (Pollard and Johnson, 1973), and further confirmed by field studies of intrusions (McColl, 1964; Jackson and Pollard, 1990; Zak and Patterson, 2006, and references therein). In addition, the lack of bedding-plane slip surfaces in the Mesozoic overburden suggests that it behaved as a single mechanical layer during the growth of the laccolith, hence increasing its resistance to bending.

According to results of experimental or numerical modelling, the basal contact of laccolithic intrusions typically extends along major flat-lying weakness zones (Roman-Berdiel et al., 1995, and references therein). In the present case, the Proterozoic–Mesozoic interface might be a plausible candidate for the floor of the Ali Sabieh laccolith. However, a shallower stratigraphic position, within the Mesozoic section, is proposed from the overburden thickness data used to construct Fig. 10a.

6. Conclusions

The magma-driven model proposed here for the Ali Sabieh antiform, at the SE periphery of the Afar plume-induced magmatic province, not only supplies new insights about strain recorded by Mesozoic and synrift layered overburden during early magmatism, but it also provides a structural understanding of a mafic magmatic complex. The so-called Ali Sabieh complex comprises, from bottom up, (i) a shallow and <2 km-thick laccolith, from which uprose (ii) a dense interdigitated sill-dyke swarm which, in turn, fed, (iii) a relatively thin (<500 m) subaerially-emplaced effusive and volcaniclastic sequence.

New K-Ar age determinations indicate that the onset of mafic magmatism in the ASR took place between 28 and 20 Ma, i.e. sligthly later than the initial basaltic trap event that occurred at ca. 30 Ma over the Ethiopian and Yemen plateaus (Hofmann et al., 1977; Coulié et al., 2003). On the other hand, the time range 28–20 Ma marks a major period of magma-assisted crustal dilatation and extension in eastern Afar *sensu lato* (Fig. 10c). It corresponds to (i) the main magmatic event recorded between 24 and 21 Ma along the Red Sea coast of Southern Arabia (Féraud et al., 1991; Sebai et al., 1991), and (ii) the main plutonic activity that occurred in Western Yemen from 22 to 21 Ma (Zumbo et al., 1995).

From a structural point of view, the Ali Sabieh antiform is assumed to have formed at an early stage of rifting in response to the emplacement of a mafic laccolith-type intrusion at shallow crustal levels, beneath a ~1 km-thick Mesozoic sedimentary cover. Our 'laccolith' model is chiefly supported by: (i) the geometry of the pluton roof, (ii) the recognition of roof pendants in the axial part of the pluton, and (iii) the mapping relationships between the main pluton, the associated dyke-sill network, the upper volcanic/volcaniclastic sequences and the various types of faults that crosscut these units. From the arched geometry of the Mesozoic overburden sequences, approximately 2 km of roof lifting was achieved, probably along reactivated transverse discontinuities. This magma-driven model is therefore inconsistent with previous hypotheses that postulated a tectonic origin in either a compressional or extensional stress regime for the antiform.

Although shallow magma chambers are commonly documented beneath axial volcanoes in most rift systems, as for example along the Icelandic rift (Bransdottir and Menke, 1992), the role of high-level intrusions in generating regional-scale folded structures in synrift cover sequences is a new hypothesis for the Afro-Arabian rift system. Syn-magmatic fold structures have been seismically imaged as small-scale domes above recent volcanoes along parts of the East African Rift System, e.g. in the Turkana rift segment, North Kenya (Dunkelman et al., 1988; Le Gall et al., 2005). The magma-driven model applied here to the ASR might supply some clues for the origin of a number of synrift antiforms, of still unknown origin, in the SE Afar rift, such as those involving the Ribta (3–4 Ma), and Mablas felsic series, north of the ASR, in the Arta transverse zone and in the DR, respectively (Fig. 1b).

Acknowledgments

This work is part of a PhD thesis (MAD) funded by the French Ministry of Foreign Affairs (*via* the CIFEG), and the CERD (Centre d'Etudes et de Recherches de Djibouti) within the framework of the MAWARI program. The authors greatly thank F. Pinard and S. Orlyk (CIFEG) for their help. Dr. M. Jalludin (Director of CERD) is also warmly acknowledged for his interest and logistical support. Many thanks are also due to 'Tony' Caminiti (CERD) for his help in the field. The text and illustrations were considerably improved according to the critical comments of Dr. A.R. Cruden and three anonymous rewievers.

Appendix. Supplementary material

Supplementary data associated with this article can be found, in the online version, at doi:10.1016/j.jsg.2010.06.007.

References

Angelier, J., 1994. Palaeostress analysis of small-scale brittle structures. In: Hancock, P. (Ed.), Continental Deformation, 4. Pergamon Press, pp. 53–100.
Annen, C., Blundy, J.D., Sparks, R.S.J., 2006. The genesis of intermediate and silicic magmas in deep crustal hot zones. Journal of Petrology 47, 505–539.
Audin, L., Quidelleur, X., Coulié, E., Courtillot, V., Gilder, S., Manighetti, I., Gillot, P.Y., Tapponnier, P., Kidane, T., 2004. Palaeomagnetism and K-Ar and ^{40}Ar-^{39}Ar ages in the Ali sabieh area (Republic of Djibouti and Ethiopia): constraints on the mechanism of Aden ridge propagation into southeastern Afar during the last 10 My. Geophysical Journal International 158, 327–345.
Barberi, F., Ferrara, G., Santacroce, R., Varet, J., 1975. Structural evolution of the Afar triple junction. In: Pilger, A., Rösler, A. (Eds.), Afar Depression of Ethiopia, vol. 1. Schweizerbart, Stuttgart, pp. 38–54.
Barberi, F., Varet, J., 1977. Volcanism in Afar: small scale plate tectonics implications. Geological Society of America Bulletin 88, 1251–1266.
Barrère, P., Boucarut, M., Clin, M., Moussie, C., Pouchan, P., Thibault, C., Weidmann, M., 1975. Carte géologique du Territoire Français des Afars et des Issas. Feuille Ali Sabieh. Bordeaux-Djibouti. Université de Bordeaux III, scale 1:100 000.
Black, R., Morton, W., Rex, D.C., 1975. Block tilting and volcanism within the Afar in the light of recent K/Ar dates. In: Pilger, A., Rösler, A. (Eds.), Afar Depression of Ethiopia, 1. Schweizerbart, Stuttgart, pp. 296–299.
Black, R., Morton, W., Varet, J., 1972. New data on Afar tectonics. Nature Physical Science 240, 170–173.
Bosworth, W., Huchon, P., McClay, K., 2005. The Red Sea and Gulf of Aden basin. Journal of African Earth Sciences 43, 334–378.

Bransdottir, B., Menke, W.H., 1992. The low-velocity zone within the Krafla caldera, NE-Iceland attributes to small magma chamber. Geophysical Research Letters 24, 2381–2384.
Cassignol, C., Gillot, P.Y., 1982. Range and effectiveness of unspiked potassium-argon dating: experimental groundwork and applications. In: Odin, G.S. (Ed.), Numerical Dating in Stratigraphy. John Wiley & Sons, Chichester, pp. 159–179.
Charbit, S., Guillou, H., Turpin, L., 1998. Cross calibration of K-Ar standard minerals using an unspiked Ar measurement technique. Chemical Geology 150, 147–159.
Chessex, R., Delaloye, M., Fontignie, D., 1979. K-Ar datations on volcanic rocks of the Republic of Djibouti. In: Geodynamic evolution of the Afro-Arabian rift system. Atti dei Convegni Lincei, Academia Nazionale dei Lincei, Roma, 47: 505–514.
Chessex, R., Delaloye, M., Muller, J., Weidmann, M., 1975. Evolution of the volcanic region of Ali-Sabieh (T.F.A.I) in the light of K/Ar age determinations. In: Pilger, A., Rösler, A. (Eds.), Afar Depression of Ethiopia, vol. 1. Schweizerbart, Stuttgart, pp. 220–227.
Clin, M., 1991. Evolution of eastern Afar and the Gulf of Tadjura. Tectonophysics 198, 355–368.
Clin, M., Pouchan, P., 1970. Carte géologique du territoire Français des Afars et des Issas. C.E.G.D, scale 1:200 000.
Corry, C.E., 1988. Laccoliths: mechanics of emplacement and growth. Geological Society of America Special Paper 220, 110.
Cotten, J., Le Dez, A., Bau, M., Caroff, M., Maury, R.C., Dulski, P., Fourcade, S., Bohn, M., Brousse, R., 1995. Origin of anomalous rare-earth element and yttrium enrichments in subaerially exposed basalts: evidence from French Polynesia. Chemical Geology 119, 115–138.
Coulié, E., Quidelleur, X., Gillot, P.Y., Courtillot, V., Lefèvre, J.C., Chiésa, S., 2003. Comparative K-Ar and Ar-Ar dating of Ethiopian and Yemenite Oligocene volcanism: implications for timing and duration of the Ethiopian traps. Earth and Planetary Sciences Letters 206, 477–492.
Cruden, A.R., McCaffrey, K.J.W., 2001. Growth of plutons by floor subsidence: implications for rates of emplacement, intrusion spacing and melt-extraction mechanisms. Physics and Chemistry of the Earth, Part A. Solid Earth and Geodesy 26, 303–315.
Deniel, C., Vidal, P., Coulon, C., Vellutini, P.J., Piguet, P., 1994. Temporal evolution of mantle sources during continental rifting: the volcanism of Djibouti (Afar). Journal of Geophysical Research 99, 2853–2869.
Dixon, J.M., Simpson, D.G., 1987. Centrifuge modelling of the laccolith intrusion. Journal of Structural Geology 9, 87–103.
Dunkelman, T.J., Karson, J.A., Rosendahl, B.R., 1988. Structural style in the Turkana rift, Kenya. Geology 16, 258–261.
Eagles, G., Gloaguen, R., Ebinger, C., 2002. Kinematics of the Danakil microplate. Earth and Planetary Science Letters 203, 607–620.
Féraud, G., Zumbo, V., Sebai, A., Bertrand, H., 1991. $^{40}Ar/^{39}Ar$ age and duration of tholeiitic magmatism related to the early opening of the Red Sea rift. Geophysical Research Letters 18, 195–198.
Gadalia, A., 1980. Les rhyolites du stade initial de l'ouverture d'un rift: exemple des rhyolites miocènes de l'Afar. Unpublished Ph. D. thesis, Université de Paris XI-Orsay, 183 pp.
Gasse, F., Varet, J., Mazet, G., Recroix, F., Ruegg, J.C., 1986. Carte géologique de la République de Djibouti. Ali Sabieh. Notice explicative. ISERST. Ministère français de la Coopération, Paris, scale 1:100 000.
Guillou, H., Singer, B., Laj, C., Kissel, C., Scaillet, S., Jicha, B.R., 2004. On the age of the Laschamp geomagnetic event. Earth and Planetary Science Letters 227, 331–343.
Hofmann, C., Courtillot, V., Féraud, G., Rochette, P., Yurgu, G., Ketefo, E., Pik, R., 1977. Timing of the Ethiopian flood basalt event and implications for plume birth and global change. Nature 389, 338–341.
Hofstetter, R., Beyth, M., 2003. The Afar Depression: interpretation of the 1960–2000 earthquakes. Geophysical Journal International 155 (2), 715–732.
Jackson, M., Pollard, D.D., 1990. Flexure and faulting of sedimentary host rocks during growth of igneous domes, Henry Mountains, Utah. Journal of Structural Geology 12, 185–205.
Le Gall, B., Vétel, W., Morley, C.K., 2005. Inversion tectonics during continental rifting. The Turkana rifted zone, Northern Kenya. Tectonics 24, TC2002. doi:10.1029/2004TC001637.
McCaffrey, K.J.W., Petford, N., 1997. Are granitic intrusions scale-invariant? Journal of the Geological Society of London 154, 1–4.
McColl, R.C., 1964. Geological and structural studies in batholithic rocks of Southern California. Part 1. Structural geology of Rattlesnake Mountain pluton. Bulletin of the Geological Society of America 75, 805–822.
Morley, C.K., Harper, R.M., Wigger, S.T., 1999. Tectonic inversion in east Africa. In: Morley, C.K. (Ed.), Geoscience of Rift Systems – Evolution of East Africa. American Association of Petroleum Geologists, Studies in Geology, vol. 44, pp. 193–210.
Muller, J., Boucarut, M., 1975. Evolution structurale de la région d'Arta-Ali Sabieh (T.F.A.I), Afrique orientale. In: Pilger, A., Rösler, A. (Eds.), Afar Depression of Ethiopia, vol. 1. Schweizerbart, Stuttgart, pp. 228–231.
Petford, N., Cruden, A.R., McCaffrey, K.W.J., Vigneresse, J.L., 2000. Granite magma formation, transport and emplacement in the Earth's crust. Nature 408, 669–673.
Pollard, D.D., Johnson, A.M., 1973. Mechanics of growth of some laccolithic intrusions in the Henry Mountains, Utah, II. Bending and failure of overburden layers and sill formation. Tectonophysics 18, 311–354.
Ring, U., Betzler, C., Delvaux, D., 1992. Normal versus strike-slip faulting during rift development in East Africa: the Malawi rift. Geology 20, 1015–1018.
Rogers, N.W., 2006. Basaltic magmatism and the geodynamics of the east African rift system. In: Yirgu, G., Ebinger, C.J., Maguire, P.K.H. (Eds.), The Afar Volcanic Province within the East African Rift System. Geological Society of London, Special Publication, vol. 259, pp. 77–93.
Roman-Berdiel, T., Gapais, D., Brun, J.P., 1995. Analog models of laccolith formation. Journal of Structural Geology 17, 1337–1345.
Rowan, M.G., 1995. Structural styles and evolution of allochthonous salt, central Louisiana outer shelf and upper slope. In: Jackson, M.P., Roberts, D.G., Snelson, S. (Eds.), Salt Tectonics: a Global Perspectives for Exploration. American Association of Petroleum Geologists Memoir, vol. 65, pp. 199–228.
Scaillet, S., Guillou, H., 2004. A critical evaluation of young (near-zero) K-Ar ages. Earth and Planetary Science Letters 220, 265–275.
Schlische, R.W., 1995. Geometry and origin of fault-related folds in extensional settings. American Association of Petroleum Geologists Bulletin 79, 1661–1678.
Sebai, A., Zumbo, V., Féraud, G., Bertrand, H., Hussain, A.G., Giannerini, G., Campredon, R., 1991. $^{40}Ar/^{39}Ar$ dating of alkaline and tholeiitic magmatism of Saudi Arabia related to the early Red Sea Rifting. Earth and Planetary Science Letters 198, 289–306.
Sperner, B., Ratschbacher, L., Ott, R., 1993. Fault-striae analysis: a turbo-pascal program package for graphical presentation and reduced stress tensor calculation. Computers and Geosciences 19 (9), 1361–1388.
Steiger, R.H., Jäger, E., 1977. Subcommission on geochronology: convention on the use of decay constants in geo- and cosmochronology. Earth and Planetary Science Letters 36, 359–362.
Varet, J., Gasse, F., 1978. Carte géologique de l'Afar central et méridional (Ethiopie et TFAI) au 1/500000, CNRS-CNR, Geotechnip, La Celle Saint-Cloud.
Vidal, P., Deniel, C., Vellutini, P.J., Piguet, P., Coulon, C., Vincent, J., Audin, J., 1991. Changes of mantle sources in the course of a rift evolution: the Afar case. Geophysical Research Letters 18, 1913–1916.
Withjack, M.O., Meisling, K.E., Russell, L.R., Tankard, A.J., Balkwill, H.R., 1989. Forced folding and basement-detached normal faulting in the Haltenbanken area, offshore Norway. In: Extensional Tectonics and Stratigraphy of the North Atlantic Margins. American Association of Petroleum Geologists Memoir, vol. 46, pp. 567–575.
Wolfenden, E., Ebinger, C., Yirgu, G., Renne, P.R., Kelley, S.P., 2005. Evolution of a volcanic rifted margin: southern Red Sea, Ethiopia. Geological Society of America Bulletin 117 (7–8), 846–864.
Yurtmen, S., Guillou, H., Orhan, O., Rowbotham, G., Westaway, R., 2002. Rate of strike-slip on the Amanos Fault (Karasu Valley, southern Turkey) constrained by K-Ar dating and geochemical analysis of Quaternary basalts. Tectonophysics 344, 207–246.
Zak, J., Patterson, S.R., 2006. Roof and walls of the Red Mountain Creek pluton, eastern Sierra Nevada, California (USA): implications for process zones during pluton emplacement. Journal of Structural Geology 28, 575–587.
Zumbo, V., Féraud, G., Vellutini, H., Piguet, P., Vincent, J., 1995. First $^{40}Ar/^{39}Ar$ dating on early Pliocene to Plio-Pleistocene magmatic events of the Afar-Republic of Djibouti. Journal of Volcanology and Geothermal Research 65, 281–295.